Article

Not peer-reviewed version

Stochastic Plantwide Optimizing Control for an Acrylic Acid Plant

Andrés Felipe Duque Amaya * , Ricardo Andres Tusso-Pinzón , Silvia Ochoa

Posted Date: 4 September 2024

doi: 10.20944/preprints202409.0351.v1

Keywords: plantwide control; stochastic plantwide optimizing control; acrylic acid

Article

Stochastic Plantwide Optimizing Control for an Acrylic Acid Plant

Andrés Duque [1,*], Ricardo Tusso-Pinzón [2] and Silvia Ochoa [1]

[1] Research Group on Simulation, Design, Control and Optimization (SIDCOP), Universidad de Antioquia, Calle 67#53-108, 050010 Medellin(ANT), Colombia

[2] Grupo de Investigación GIEMA,Facultad de Ciencias Básicas, Universidad Santiago de Cali, Cali 760035, Colombia

* Correspondence: andres.duquea@udea.edu.co

Abstract: This work addresses the relevant control system design issue for an acrylic acid plant through the lens of plant-wide stochastic optimization control (S-PWOC). The S-PWOC framework involves stochastic optimization methods. An evaluation comparison between the proposed S-PWOC model and two conventional models, specifically the two-level identification method and the typical plant-wide decentralized control structure, is performed. Despite the increasing computational demands associated with S-PWOC, experimental results highlight its effectiveness in handling different forms of uncertainty. Notably, S-PWOC demonstrates improvements in economic viability, control efficiency, and reduction of safety risks during plant operations.

Keywords: plantwide control; stochastic plantwide optimizing control; acrylic acid

---

1. Introduction

Chemical industries have had a significant impact on human lives through the production of essential goods and services. Since the advent of automated control systems, decentralized architecture has become the dominant approach to managing the complexity of controlling entire chemical plants [1]. This architectural structure consists of multiple PID control loops responsible for maintaining controlled variables at predetermined setpoints in each operating unit. These controllers function autonomously, regulating their designated process segments without information exchange. Implementing a traditional decentralized control structure necessitates an initial optimal process design phase.

Although optimal operation is projected at the design-phase operating point, inevitable disturbances and uncertainties can alter process conditions, potentially shifting the optimal operating parameters. The failure to recognize the existence of disruptions and uncertainties can significantly impact profitability and process safety. Therefore, managing uncertainty in the context of economic optimization is a key challenge in process control today [2]. As a result, decisions made within a robust plant-wide control (PWC) framework require careful consideration of uncertainties. Solutions failing to mitigate uncertainty impacts can compromise economic efficiency and control effectiveness, potentially resulting in unsafe and financially detrimental conditions [3].

This study proposes a comprehensive approach to solve the ship problem while considering uncertainties, called Stochastic Plant-Wide Optimization Control (S-PWOC), this method builds on previous research (Duque et al., 2021; Ochoa et al., 2010b), integrating the Economic viability and process safety considerations to improve control system design. This framework addresses dynamic stochastic real-time optimization (D-RTO), emphasizing economic profit as the primary control objective.

The proposed method is being validated using the acrylic acid production process as a case study. This choice is based on the paramount importance of this process in the chemical industry, coupled with its inherent safety concerns, making it particularly suitable for evaluating the

Preprints.org (www.preprints.org) | NOT PEER-REVIEWED | Posted: 4 September 2024 doi:10.20944/preprints202409.0351.v1

effectiveness of the proposed S-PWOC framework. Market forecasts project the global acrylic acid industry to reach USD 20.19 billion by 2027. [6], due to the increasing demand for superabsorbents, thus increasing production of acrylic acid worldwide. Notably, there is a growing demand for superabsorbent polymers in applications such as adult urinary incontinence, water treatment additives, and radioactively cured coatings, especially in low-cost economies, in emerging regions such as the Asia-Pacific region, Central America and South America, are poised to increase demand for acrylic acid ("ICIS.com web site," 2023).

Forecasts predict a global production volume of 9 million tons by 2025, driven by the rise of global industrialization and the expansion of acrylic acid applications in various sectors [8]. Therefore, coordinated research efforts targeting process control and optimization are required to improve the economic viability of acrylic acid production in the face of inherent uncertainty. The PWC formula accounts for three primary uncertainty sources: external disturbances, market fluctuations, and model parameter variations.

The following sections of this manuscript are described as follows. Section 2 comprehensively presents the theoretical foundations related to whole-process control (PWC) strategies and stochastic optimization methods. Part 3 outlines the details of the process, describes the identified safety risks, and explains the nuances of the Aspen Plus model specified to the acrylic acid (AA) process. In section 4, the Stochastic Plantwide Optimization Control (S-PWOC) method is implemented to control an acrylic acid production plant. Section 5 attempts to compare the effectiveness of the proposed S-PWOC approach to resolve the uncertainties associated with the decentralized PWC architecture and the deterministic PWOC approach. Finally, Section 6 summarizes the conclusions drawn and provides recommendations for future efforts.

2. Theoretical Background and Methods

This section summarizes the main areas explored in this work: plant-wide controls (PWCs) and the application of stochastic optimization to reduce uncertainty.

2.1. Plantwide Control Methodologies

Economic and safety imperatives, coupled with increased mass and power integration, have heightened the significance of plant-wide control (PWC) strategies in chemical plants [9]. This study proposes a control structure design method that optimizes process economics, ensures safety, and mitigates various uncertainty sources.

The PWC method designs a comprehensive plant control system, explicitly accounting for inter-unit process interactions. [10]. The basic study of PWC was introduced by Buckley in 1964 [11], and after the early 1990s many works emerged. These methods can be systematically classified into two main approaches: approach-based and structure-based [10]. Classifications of control methods can be based on approach or structure. Approach-based classifications include heuristic process-oriented, mathematical model-oriented, optimization-based, and mixed methods. Structure-based classifications comprise decentralized, distributed, centralized, and multi-layer control systems. [12]

Distributed model predictive control (MPC) systems use multiple MPCs to exchange information to achieve control goals. There are two main architectures: communication-based and collaboration-based. In the first, each MPC uses a local objective function. The exchange of information facilitates coordination while still emphasizing local goals. The second modifies local MPC objective function to incorporate system-wide control objectives. This promotes coordinated optimization across all MPCs [13]. Another popular distributed architecture is multilayer architecture. Here there is a hierarchy with at least two layers: The optimization layer, that performs high-level calculations and sets general goals. The control layer executes control actions based on directives from the optimization layer. Coordination between layers may or may not be implemented [14]. Recent applications of this architecture can be found in the work of [15–20]. In contrast, single-layer architecture uses a centralized approach. A single controller optimizes monitoring of goals, economic objectives, or a combination of both [21]. Examples of this architecture can be found in the work of [22–26].

2.2. Stochastic Optimization

George Box [27] posited that "all models are wrong, but some are useful," implying inherent model inconsistency and internal uncertainty in any modeling approach. Conservation equations in process modeling often rely on empirical parameters and material recycling, while interactions between process flows introduce uncertainties. These factors contribute to discrepancies between predicted and actual plant conditions. Additionally, fluctuations in raw material and product costs can significantly impact the process's profitability and economic viability [28]. When applying deterministic optimization solutions to real plants, inherent uncertainties can lead to suboptimal decision variables. This may result in lower-than-expected economic profitability or violation of critical process constraints. Consequently, incorporating uncertainty into optimization models is crucial for mitigating the effects of both known and unknown process perturbations in industrial applications. The S-PWOC framework introduced in this study distinguishes itself by incorporating multiple uncertainty sources within its optimization problem formulation. Certain significant stochastic programming applications in process optimization are constrained to operations involving no more than three units and solely address internal uncertainties. An example can be found in the Navia study [29]. The study conducts a comparative analysis of two-stage and random constraint optimization approaches for a hydrodesulfurization process comprising two fixed-bed reactors and a flash tank. The absence of recycle streams between process units minimizes operational disruptions and simplifies simulation models. Another example is the work of Lucia et al [3,30], which implemented a multistep NMPC strategy to optimize a semi-batch polymerization reactor. This study findings affirm the efficacy of multistage optimization in addressing model uncertainty. [31] advanced process engineering by applying random constraint optimization to a hydroformylation process comprising a CSTR reactor and a multiphase separator. In this study, the authors present the limitations of random constraint programming for application to large-scale systems and show that infeasible solutions can be found when the optimization problem formulation includes many random constraints. Stochastic constraint programming exhibits limitations in addressing large-scale systems. Furthermore, the introduction of numerous random constraints into the optimization problem formulation frequently leads to infeasible solutions. Other important studies using stochastic programming for PSE applications are on planning energy-intensive processes using electricity prices as an external uncertainty source [32] and on endogenous production uncertainties for shale gas infrastructure planning [33]. Recent studies include using two-stage stochastic programming problems to deal with uncertainties under operating conditions [34–36]. Approaches a multiscale flexibility constraints and uncertainties in refinery hydrogen systems, considering the parameter uncertainties, and proposes a CCPO (Chance Constrained Policy Optimization) algorithm to ensure that a common random constraint on the photogeneration of phycocyanin is satisfied Sharma et al. [37] used a multi-objective randomly constrained hierarchical optimization approach for production planning problems.

Despite the recognition that uncertainties are one of the primary factors driving chemical processes away from expected optimal operation, no formal PWC methodology explicitly addressing uncertainties has been proposed, to the authors' knowledge. Managing these uncertainties within the context of constantly changing market conditions and stringent safety constraints remains a significant challenge in process control and optimization [38]. In a PWC approach, uncertainty management is crucial for effective decision-making. Neglecting to address uncertainties can degrade both economic performance and process control, potentially resulting in unsafe operations and financial losses.

3. Acrylic Acid Process

The S-PWOC methodology proposed in this work is implemented to the control of a complete Acrylic Acid (AA) production plant. Although there are multiple methods for producing AA, the most employed technology at a commercial scale is the partial oxidation of propylene [39]. The process is governed by the following reactions:

Main reaction:

$$R1:\ C_3H_6 + \frac{3}{2}O_2 \ \rightarrow C_3H_4O_2 + H_2O$$

Side reactions:

$$R2:\ C_3H_6 + \frac{5}{2}O_2 \ \rightarrow C_2H_4O_2 + H_2O + CO_2$$

$$R3:\ C_3H_6 + \frac{9}{2}O_2 \ \rightarrow 3CO_2 + 3H_2O$$

Where the rate of each reaction i is:

$$-r_i = k_{0i} \exp\left(\frac{-E_{Ai}}{RT}\right) P_{O2}P_{C3H6} \quad (1)$$

The production of acrylic acid consists of two primary phases: reaction and purification. During the reaction phase, propylene oxidation yields acrylic acid alongside byproducts including acetic acid, carbon dioxide, and water. The subsequent purification phase isolates and refines acrylic acid to achieve 99.5% mole fraction purity. Figure 1 presents the P&ID diagram for the AA process under consideration, which includes several control loops integral to the decentralized PWC architecture. This decentralized PWC architecture was developed based on Suo recommendations [40] and detailed process knowledge.

The acrylic acid production plant consists of a reactor (R-101), a flash drum (T-101), an absorber (T-102), an azeotropic distillation column (T-103), and a rectification column (T-104). Propylene and air streams are fed into the reactor, where reactions R1, R2, and R3 occur. The effluent stream from the reactor (F5) is directed to the flash drum (V-101) for vapor-liquid separation. The gas stream exiting the flash drum (F7) is fed into the absorber (T-102), where AA and ACE are recovered using a solvent primarily composed of liquid water (F18). The effluent streams from the flash drum and absorber, primarily comprising acrylic acid (AA), acetic acid (ACE), and water, enter the azeotropic distillation column (T-103). Here, toluene serves as an organic solvent, exploiting the toluene-water azeotrope to extract water. The resulting liquid stream then proceeds to the rectification column (T-104), where AA is separated as the bottom product and ACE as the distillate.

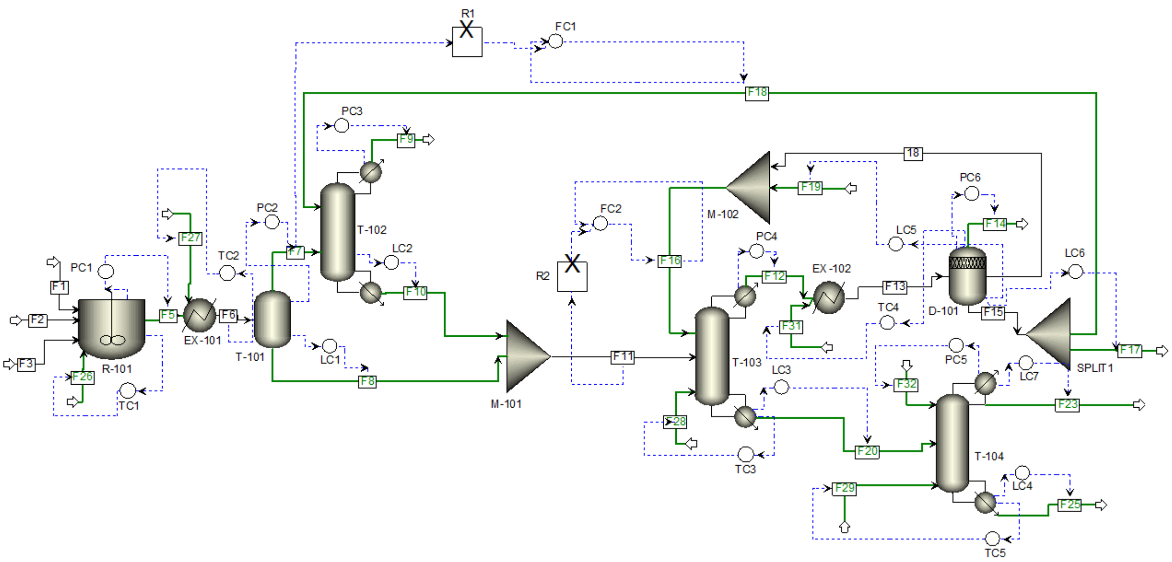

Figure 1. P&ID Diagram for AA Production: Control loops highlighted in green represent the decentralized PWC structure.

3.1. Process Modeling and Simulation

The following section provides a detailed description of the Acrylic Acid (AA) Plant model implemented in Aspen. The NRTL-HOC framework was employed for phase equilibrium calculations, with parameters sourced from [40]. Air compression was conducted using a single-stage compressor, represented by the MCompr block. The reaction section, denoted as R-101, was modeled with the RCSTR block. The kinetic expressions for reactions R1 through R3 were implemented using the power law form, with kinetic parameters sourced from [41].

A large heat exchanger is incorporated within the reactor to dissipate the substantial heat generated by the reactions. The separation section includes a flash drum, an absorber, an azeotropic distillation column, and a rectification column. The rectification column (T-103) was specified similarly to the absorber and azeotropic columns using the RadFrac block, but with both condenser and reboiler configurations. For the simulation, two tear streams were generated, and the Wegstein method was selected for recycle convergence.

In the dynamic simulation, equipment such as valves and pumps are specified. The parameters required for dynamic simulation are detailed in Table 2 in the supporting information. After achieving steady-state simulation of the plant in Aspen Plus and inputting the necessary parameters for dynamic simulation, the files were exported to Aspen Dynamics. Basic P&ID controllers were added and tuned in accordance with the Tyreus-Luyben rules [42,43].

Parameters and simulation data for both steady-state and dynamic simulations are provided in the supporting information section. Nominal operating conditions for the AA plant were sourced from Suo et al. [40] and Turton et al. [39]. The flash separation process (V-101) was modeled using the Flash2 block, and the absorption process (T-101) was simulated using the RadFrac block, configured without specifying a condenser or reboiler. The azeotropic distillation column (T-102) is modeled using the RadFrac block, configured with a reboiler but no condenser. To achieve complete separation of water and toluene, a condenser (E-102) and a decanter (D-101) are necessary. The decanter is simulated using the H-Drum block, which has three specified outlets: one for the vapor stream and two for the aqueous and organic phases.

3.2. Safety Risks during Plant Operation

The successful implementation of the S-PWOC framework within the acrylic acid production plant necessitates a thorough identification and integration of safety risks into the stochastic programming formulation. A comprehensive analysis of the process, coupled with a review of pertinent literature on acrylic acid production, has highlighted two critical areas of concern with potentially significant impacts.

The flammability limits of propylene in the presence of oxygen pose a significant risk. According to Turton et al. [39], it is crucial to keep oxygen levels below 5 mol% during the reaction stage to mitigate this hazard.

Secondly, the highly exothermic nature of acrylic acid polymerization poses another critical risk [40]. Acrylic acid tends to dimerize at temperatures exceeding 110°C, necessitating strict temperature controls at the bottoms of distillation columns to prevent incidents.

To ensure the safe operation of the acrylic acid plant, these identified risks must be explicitly formulated as constraints within the S-PWOC framework as follows:

$$x_{O2,5}\left(t_0 + \Delta t_{opt}, u_{PW}\right) < 0.05 \qquad \left[\frac{kmol}{kmol}\right] \qquad (2)$$

$$T_{Reb,20}\left(t_0 + \Delta t_{opt}, u_{PW}\right) < 110 \qquad [°C] \qquad (3)$$

$$T_{Reb,24}\left(t_0 + \Delta t_{opt}, u_{PW}\right) < 110 \qquad [°C] \qquad (4)$$

4. Stochastic Optimization of Acrylic Acid Production: Managing Uncertainties in Plantwide Control

The proposed SPWOC approach is a framework that improves the PWOC methodology, proposed in [44] , by including explicitly different sources of uncertainty. The proposed S-PWOC framework is implemented for the acrylic acid process, described in Section 3. Finally, a comparison between the proposed S-PWOC, a deterministic P-WOC approach and a decentralized PWC structure is presented. The proposed Stochastic Plantwide Optimal Control (PWOC) methodology comprises six sequential steps, as illustrated in Figure 2. In the present work, design of step1 is achieved according with process knowledge. In several PWC methodologies process knowledge is important for taking decisions [1,9,45–50].

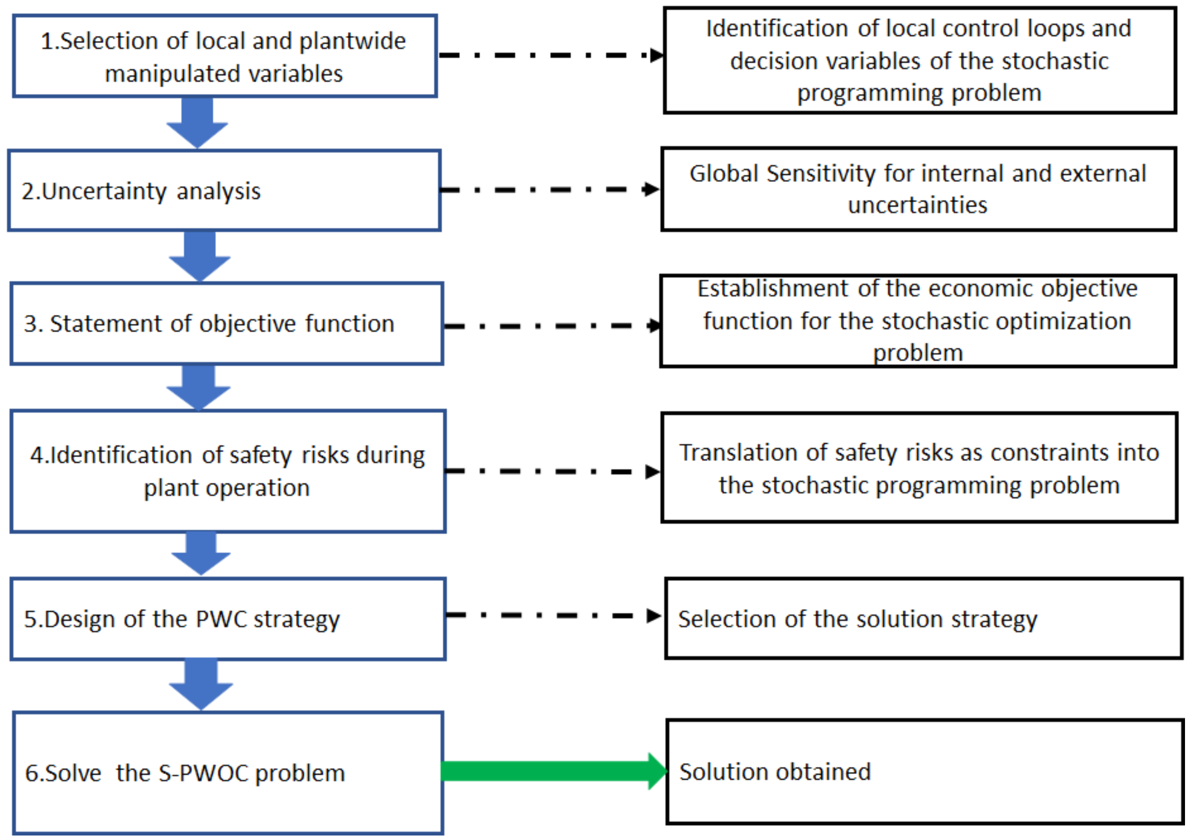

Figure 2. Stages of the Stochastic-PWOC strategy.

As follows, each stage of the S-PWOC framework is given, specifically applied to the Acrylic Acid process case study. The proposed steps provide a roadmap for formulating and addressing the resulting Stochastic The optimization problem aims to achieve a balanced integration of economic considerations and control objectives while ensuring the safe operation of the plant. The general approach illustrated in Figure 2 is applicable to various other applications.

Stage 1. Selection of local and plantwide manipulated variables

The local control strategy must ensure the safe operation of equipment during plant processes. Typically, these local control loops encompass level and pressure control objectives. The primary aim of this strategy is to maintain the controlled variables at their predefined set-points. To achieve this objective, local manipulated variables (u_{loc}) are selected based on process knowledge.

Following the closure of local control loops, the remaining manipulated variables are identified as plantwide manipulated variables (u_{PW}). These plantwide manipulated variables serve as decision variables in the resulting stochastic programming problem formulation. Table 1 illustrates the pairing of local control loops and the plantwide manipulated variables employed to enhance the economic profitability of the process. This selection is grounded in process knowledge and aligns with the recommendations of Suo et al. [40] and Turton et al. [39].

Figure 3 visually distinguishes local control loops and plantwide manipulated variables, depicted in green and red respectively. Moreover, PI controllers were fine-tuned using Tyreus-Luyben correlations to optimize control performance.

Table 1. Selection of local and plantwide manipulated variables.

Manipulated Variables at Local Level	Manipulated variables at Plantwide level

Liquid flowrate (F8) for controlling liquid level in flash(V-101)	Flowrate of air at reactor inlet (F_1)
Liquid flowrate(F10) for controlling liquid level in absorber(T-101)	Flowrate of propylene at reactor inlet (F_3)
Liquid steam (F20) to control the liquid level in the azeotropic column (T-102)	Steam flowrate at the reactor inlet (F_2)
Liquid steam (F25) to control the liquid level in the rectification column(T-103)	Reactor utility flowrate (F_{26})
Liquid steam (F19) to control the liquid organic level in decanter(D-101)	Heat exchanger E-101 utility fluid flowrate (F_{27})
Liquid steam (F17) to control the liquid water level in decanter(D-101)	Heat exchanger E-102 utility fluid flowrate (F_{31})
Liquid steam of distillate (F23) to control the liquid level for reflux drum (V-102) in rectification column	Steam of aqueous phase recycled into the absorber column (F_{18})
Vapor steam (F5) to control the pressure in the reactor (R-101)	Steam of organic phase recycled into the azeotropic column (F_{16})
Vapor steam (F7) to control the pressure in flash drum (V-101)	Steam of utility fluid in the reboiler azeotropic column (F_{28})
Vapor flowrate (F9) for controlling pressure in absorber (T-101)	Reflux rate in the rectification column (F_{30})
Vapor flowrate(F12) for controlling pressure in azeotropic column(T-102)	Flowrate of utility fluid used in reboiler rectification column (F_{29})
Utility fluid flowrate(F32) used in E-105 heat exchanger for controlling pressure in rectification column(T-103)	
Vapor flowrate(F14) for controlling pressure in decanter(D-101)	

 doi:10.20944/preprints202409.0351.v1

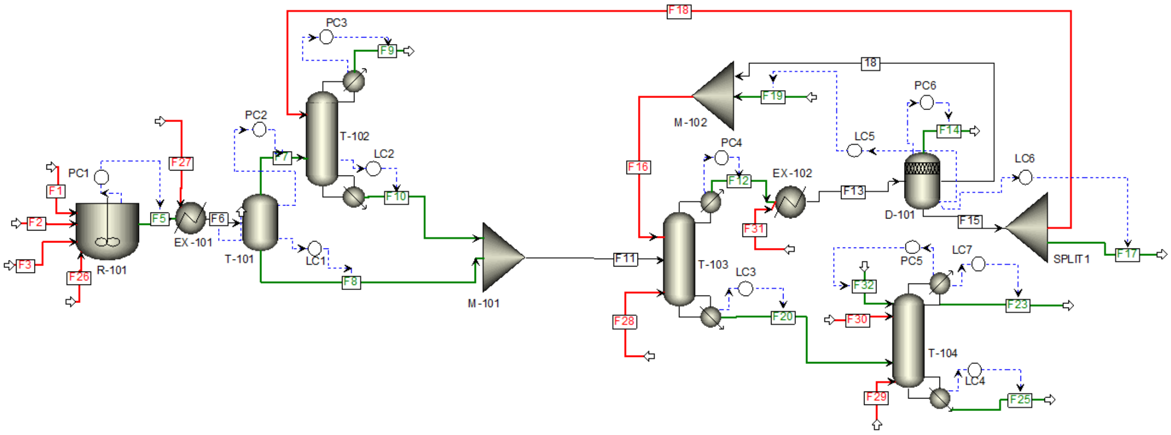

Figure 3. Local control loops implemented for acrylic acid production. Streams in red correspond to the streams used as plantwide manipulated variables.

Stage 2. Uncertainty analysis

In this stage, the effects of uncertainties in the plant are described and quantified. Three primary sources of uncertainty are identified: internal, external, and process uncertainty [31]. Internal uncertainty pertains to model errors arising from parameters derived from experimental data, such as kinetic constants, physical properties, and transfer coefficients. External uncertainties involve external events impacting the process performance, including fluctuations in the costs of raw materials and products, variations in environmental conditions, and inconsistencies in the quality of raw materials. Process uncertainties refer to disturbances within the process itself, such as variations in stream composition, temperatures, and pressures. To effectively identify the principal sources of uncertainty affecting a specific process, it is recommended to integrate process knowledge with a sensitivity analysis.

The selected set of uncertain variables is incorporated into the S-PWOC scheme to derive optimal trajectories that mitigate the effects of uncertainty on the process. In the acrylic acid production process, the primary internal uncertainties are encapsulated in six key variables: the activation energies for the three reactions (E_{A1}, E_{A2}, E_{A3}) and the pre-exponential kinetic factors (k_{01}, k_{02}, k_{03}). These parameters, derived from experimental studies, significantly influence both the molar production of acrylic acid (AA) and the economic objective function.

External uncertainties that have a substantial impact on the economic objective function include the prices of acrylic acid, acetic acid, and propylene. These external factors are crucial as they directly affect the cost and profitability of the production process. By considering both internal and external uncertainties, the S-PWOC scheme enables the optimization of process trajectories, thereby enhancing the robustness and efficiency of acrylic acid production.

Tables 2 and 3 present the results of a global sensitivity analysis for internal uncertainties, calculated using a normalized linear regression. The limit values for activation energies and pre-exponential parameters were sourced from acrylic acid kinetic studies conducted by [51]. Table 4 displays the results of the global sensitivity analysis for external uncertainties. The limit values for the prices of acrylic acid, propylene, and acetic acid were obtained from a chemicals market website ("ICIS.com web site," 2023). Additionally, the temperature of air at the reactor inlet is considered as a process uncertainty, representing a disturbance.

These three types of uncertainties—internal, external, and process—are utilized to evaluate the performance of the proposed S-PWOC framework. This comprehensive analysis enables a robust assessment of the framework's efficacy in mitigating the impact of uncertainties on the acrylic acid production process.

Table 2. Global Sensitivity for internal uncertainties: activation energy parameters.

 doi:10.20944/preprints202409.0351.v1

Description	E_{A1} (kJ/kmol)	Profit (USD/h)	E_{A2} (kJ/kmol)	Profit (USD/h)	E_{A3} (kJ/kmol)	Profit (USD/h)
Lower Limit	13927,02	12300,00	16718,90	4537,30	18602,80	4664,50
Nominal Value	15000,00	9248,20	20000,00	9248,20	25000,00	9248,20
Upper Limit	16072,97	1186,70	23281,07	9769,20	30397,20	10680,54
Average	15000,00	7578,30	19999,99	7851,57	24666,67	8197,75
Slope	-5,18		0,80		0,52	
Global sensitivity index	**10,25**		**2,03**		**1,55**	

Table 3. Global Sensitivity for internal uncertainties: kinetic constants parameters.

Description	k_{01} (kJ/kmol. s)	profit (USD/h)	k_{02} (kJ/kmol. s)	profit (USD/h)	k_{03} (kJ/kmol. s)	profit (USD/h)
Lower Limit	3,09E-05	8679,82	1,72E-04	10591,45	0,04	11524,28
Nominal Value	4,42E-05	9248,20	2,45E-04	9248,20	0,05	9248,20
Upper Limit	5,74E-05	11510,91	3,19E-04	10363,33	0,07	9475,43
Average	4,42E-05	9812,98	2,45E-04	10067,66	0,05	10082,64
Slope	106752654,31		-1513891,22		-67842,72	
Global sensitivity index	**0,48**		**0,04**		**0,34**	

Table 4. Global Sensitivity analysis for external uncertain parameters.

Description	AAprice (USD/kmol)	Profit (USD/h)	ACEprice (USD/kmol)	Profit (USD/h)	C_3H_6price (USD/kmol)	Profit (USD/h)
Lower Limit	121,233	4382,7	62,958	9094,6	38,9130	11402,5
Nominal Value	173	9248,2	89,94	9248,2	55,59	9248,2

Preprints.org (www.preprints.org) | NOT PEER-REVIEWED | Posted: 4 September 2024 doi:10.20944/preprints202409.0351.v1

Upper Limit	225,147	14222,5	116,922	9473,8	72,267	7166,2
Average	173,216	9284,47	89,949	9272,20	55,59	9272,30
Slope	0,02		1,81E-03		7,90E-03	
Global sensitivity index	**0,25**		**0,01**		**0,13**	

From the global sensitivity results for internal uncertain parameters (Tables 2 and 3) we can observe that the activation energy for the first reaction (E_{A1}) presents the largest impact on the total economic profit. Similarly, Table 4 shows that the price of the acrylic acid (main product), has the highest impact on the profit objective function. Therefore, these two are considered in the set of random variables Ξ. Uncertainty evolution is represented using lower, nominal an upper value, and decision variables counteract the effects of uncertainty in the considered interval. A robust horizon of two is considered for simplicity and reduction in computing time. This means branching the tree until stage two, afterwards constant values are considered for the uncertainties. This strategy is employed to avoid the exponential growth of the scenario tree with the prediction horizon. The main idea of this simplification is that due to the receding horizon nature of NMPC, modeling the far future very accurately is not critical because all the control inputs will be recomputed at the next sampling time [3].

Stage 3. Statement of objective function

In this work, multistage programming is employed to handle uncertainties and formulate the corresponding Stochastic PWOC problem. Decision variables, states, and constraints are represented across multiple stages. At each decision stage, the objective function is maximized based on the values of the random variables $\xi \in \Xi$. Equation (5) defines the economic objective function for the acrylic acid production plant under conditions of uncertainty:

$$\varphi = \sum_{i=1}^{n} \omega_i J_i({x_{k+1}}^j, {u_k}^j) \qquad (5)$$

In this context, φ represents the expected economic objective function of the plant. The term ω_i denotes the probability of occurrence for each scenario i, while n is the total number of scenarios or leaf nodes considered. The cost associated with each scenario, $J_i({x_{k+1}}^j, {u_k}^j)$, is defined by Equation (6):

$$\begin{aligned} J_i({x_{k+1}}^j, {u_k}^j) = \sum_{k=1}^{N} & {w_1}^j {F_{AA25,k+1}}^j + {w_2}^j {F_{ACE23,k+1}}^j - {w_3}^j {F_{1,k+1}}^j - {w_4}^j {F_{2,k+1}}^j - {w_5}^j {F_{3,k+1}}^j \\ & - {w_6}^j {F_{19,k+1}}^j - {w_7}^j {F_{26,k+1}}^j - {w_8}^j {F_{27,k+1}}^j - {w_9}^j {F_{28,k+1}}^j - {w_{10}}^j {F_{29,k+1}}^j \\ & - {w_{11}}^j {F_{31,k+1}}^j \end{aligned} \qquad (6)$$

In this formulation, ${w_i}^j$ represents cost factors obtained from a chemicals market website ("ICIS.com web site," 2023). The first and second terms in Equation (6) account to produce acrylic acid and acetic acid at stage $k+1$ for each scenario j. The subsequent three terms, weighted by w_3, w_4, and w_5, consider the costs of raw materials—air, propylene, and steam—at stage $k+1$ for each scenario j.

The term weighted by w_6 accounts for toluene makeup in the decanter at stage $k+1$ for each scenario j. Additionally, terms weighted by w_7, w_8, w_9, w_{10}, and w_{11} impose penalties for energy consumption associated with utility fluids in the reactor and heat exchangers E-101, E-103, E-106, E-105, and E-102 at stage $k+1$ for each scenario j The economic objective function for each scenario i is computed over a prediction horizon N.

Stage 4. Identification of safety risks during plant operation

The incorporation safety risks as constraints in the S-PWOC formulation is essential to ensure the safe operation of the process during multistage economic optimization. This objective is achieved by imposing limitations on states and manipulated plant-wide variables, thereby balancing economic performance, control, and process safety. For the acrylic acid process, these constraints must be satisfied across all scenarios within the S-PWOC framework.

$$x_{O2,k}{}^{j} < 0.05 \qquad [\frac{kmol}{kmol}] \tag{7}$$

$$T_{Reb20,k}{}^{j} < 110 \qquad [°C] \tag{8}$$

$$T_{Reb24,k}{}^{j} < 110 \qquad [°C] \tag{9}$$

The first constraint aims to prevent a reactor explosion, which could occur if the oxygen composition exceeds 5% by mole. The second and third constraints limit the bottom temperatures in the azeotropic and rectification columns to prevent acrylic acid polymerization. Constraints (7) to (9) must be satisfied when solving the S-PWOC formulation at stage k k for each scenario j.

Stage 5. Design of PWC architecture

The performance of the proposed S-PWOC approach is compared against a deterministic PWOC and a typical decentralized PWC structure to assess the impact of incorporating uncertainties in a PWC formulation. Although achieving a robust solution increases computational time demands, the resulting improvement in economic profitability justifies this trade-off. Robust optimization, such as min-max NMPC, is another strategy for handling uncertainties; however, it was not selected due to its tendency to yield conservative solutions by optimizing for the worst-case scenario [30].

For the implementation of the S-PWOC, a two-layer PWC structure was employed instead of a single-layer structure. This choice is based on the proven stability of the two-layer structure in rejecting disturbances [52] and its ability to satisfy constraints across all scenarios, leveraging the nature of multistage NMPC [3,30]

To manage various sources of uncertainties and ensure a balance between economic performance, control, and safe operation, the use of a multilayer architecture is recommended at this stage. The formulation of a multilayer stochastic programming problem that includes diverse sources of uncertainty, such as model mismatches, market conditions, and process disturbances, is a novel approach from a PWC perspective.

Until now, stochastic programming approaches have primarily been applied within single-layer control architectures and have focused solely on addressing model mismatches in chemical processes [3,30,53–56]. The general implementation scheme proposed involves two main layers: the optimization layer and the control layer. In the optimization layer, a Dynamic Real-Time Optimization (D-RTO) problem under uncertainties is solved to maximize the economic profitability of the process.

The optimization layer provides optimal plant-wide manipulated variables and state trajectories, which are then sent as set-points to the regulatory control layer. This regulatory control layer comprises a multistage Nonlinear Model Predictive Control (NMPC) system, which predicts future process operations and tracks the set points provided by the optimization layer. The optimal decision variables determined by the multistage NMPC are subsequently applied to the actual plant. The Dynamic Real-Time Optimization (D-RTO) problem solved in the optimization layer is defined by Equation (10):

$$\begin{aligned}
&\max_{u_k{}^{j}(opt)\ \forall (j,k)\in I} \sum_{i=1}^{n} w_i J_i(x_{k+1}{}^{j}, u_k{}^{j}) \\
&s.to.\ x_{k+1}{}^{j} = f\left(x_k{}^{p(j)}, u_k{}^{j}, \xi_k{}^{r(j)}\right) \\
&u_{min} \le u_k{}^{j} \le u_{max} \\
&F_{25,k}{}^{j} \ge 70.96 \qquad [\frac{kmol}{h}] \\
&x_{AA25,k}{}^{j} \ge 0.995 \qquad [\frac{kmol}{kmol}] \\
&x_{O2-5,k}{}^{j} < 0.05 \qquad [\frac{kmol}{h}] \\
&T_{Reb20,k}{}^{j} < 110 \qquad [°C]
\end{aligned} \tag{10}$$

 doi:10.20944/preprints202409.0351.v1

$T_{Reb24,k}{}^{j} < 110 \qquad [°C]$
$u_k{}^{j} = u_k{}^{l} \;\; if \;\; x_k{}^{p(j)} = x_k{}^{p(l)}$

The vector $u_k{}^{j}(opt)$ is the solution to the D-RTO problem, providing optimal decision variables for each scenario j. The cost function for each scenario, J_i, represents the economic profit of the process and is defined by Equation (6). Each state $x_{k+1}{}^{j}$ depends on the previous state $x_k{}^{p(j)}$, the control decision variable $u_k{}^{j}$, and the realization r of the uncertainty $\xi_k{}^{r(j)}$.

The second constraint delineates the search space for decision variables during optimization. The third constraint, for $F_{25,k}{}^{j}$, is a productivity requirement. The fourth constraint, for $(x_{AA25,k}{}^{j})$, ensures the required product purity of acrylic acid. From the fifth to the last constraint, safety risks for plant operation must be satisfied. The final constraint is the non-anticipative constraint, which stipulates that states with the same parent node must share identical decision variable profiles.

$$
\begin{aligned}
&\min_{u_k{}^{j}(NMPC)\,\forall(j,k)\in I} \sum_{i=1}^{n} \omega_i J_{Tracki} \\
&s.to.\; x_{k+1}{}^{j} = f\left(x_k{}^{p(j)}, u_k{}^{j}, \xi_k{}^{r(j)}\right) \\
&u_{min} \le u_k{}^{j} \le u_{max} \\
&F_{25,k}{}^{j} \ge 70.96 \qquad [\frac{kmol}{h}] \\
&x_{AA25,k}{}^{j} \ge 0.995 \qquad [\frac{kmol}{kmol}] \\
&x_{O2-5,k}{}^{j} < 0.05 \qquad [\frac{kmol}{kmol}] \\
&T_{Reb20,k}{}^{j} < 110 \qquad [°C] \\
&T_{Reb24,k}{}^{j} < 110 \qquad [°C] \\
&u_k{}^{j}(NMPC)(t_0) = u_k{}^{j}(opt)
\end{aligned} \tag{11}
$$

In the multistage NMPC layer, the optimization problem formulation is given by Equation (11). Here, ω_i represents the probability of occurrence for each scenario, $x_{k+1}{}^{j}$ is the vector of predicted states at stage $k+1$, and the constraints hold the same meanings as in Equation (10), except for the last one. The final constraint assigns the initial conditions for the decision variables of the NMPC layer to the optimal profiles $u_k{}^{j}(opt)$ calculated by the optimization layer. The cost function for each scenario, J_{Tracki}, represents a tracking objective function that penalizes deviations of state variables from their optimal values calculated in the optimization layer, as well as penalizes control movements to ensure smooth operation.

$$
\begin{aligned}
J_{Tracki} = &\sum_{k=1}^{N} Q_1(T_{k+1}{}^{j} - T_{sp})^2 + R_1\left[F_{1k}{}^{j} - F_{1k}{}^{j}(opt)\right]^2 + R_2\left[F_{2k}{}^{j} - F_{2k}{}^{j}(opt)\right]^2 \\
&+R_3\left[F_{3k}{}^{j} - F_{3k}{}^{j}(opt)\right]^2 + R_4\left[F_{26k}{}^{j} - F_{26k}{}^{j}(opt)\right]^2 + R_5\left[F_{27k}{}^{j} - F_{27k}{}^{j}(opt)\right]^2 \\
&+R_6\left[F_{18k}{}^{j} - F_{18k}{}^{j}(opt)\right]^2 + R_7\left[F_{16k}{}^{j} - F_{16k}{}^{j}(opt)\right]^2 + R_8\left[F_{28k}{}^{j} - F_{28k}{}^{j}(opt)\right]^2 \\
&+R_9\left[F_{30k}{}^{j} - F_{30k}{}^{j}(opt)\right]^2 + R_{10}\left[F_{29k}{}^{j} - F_{29k}{}^{j}(opt)\right]^2 + R_{11}\left[F_{31k}{}^{j} - F_{31k}{}^{j}(opt)\right]^2 \\
&+P_1\left(\Delta F_{1k}{}^{j}\right)^2 + P_2\left(\Delta F_{2k}{}^{j}\right)^2 + P_3\left(\Delta F_{3k}{}^{j}\right)^2 + P_4\left(\Delta F_{26k}{}^{j}\right)^2 + P_5\left(\Delta F_{27k}{}^{j}\right)^2 + P_6\left(\Delta F_{18k}{}^{j}\right)^2 \\
&+P_7\left(\Delta F_{16k}{}^{j}\right)^2 + P_8\left(\Delta F_{28k}{}^{j}\right)^2 + P_9\left(\Delta F_{30k}{}^{j}\right)^2 + P_{10}\left(\Delta F_{29k}{}^{j}\right)^2 + P_{11}\left(\Delta F_{31k}{}^{j}\right)^2
\end{aligned} \tag{12}
$$

As delineated in equation (12), penalization terms are implemented to address deviations of both temperature and plantwide manipulated variables from their optimal values, as determined by the optimization layer. The plantwide manipulated variables, previously defined in stage 2, encompass the following parameters:

1. The volumetric flow rate of air, (F_1);
2. The mass flow rate of propylene, (F_2);
3. The mass flow rate of steam, (F_3);
4. The flow rate of utility fluid circulated through the reactor jacket, (F_{26});
5. The flow rate of utility fluid utilized in heat exchangers E-101 and E-102, (F_{27}, F_{31});
6. The flow rate of recycled water introduced into the absorber column, (F_{18});
7. The flow rate of organic phase recycled into the azeotropic column, (F_{16});
8. The flow rate of utility fluid employed in the reboiler of the azeotropic column, (F_{28}); and

 doi:10.20944/preprints202409.0351.v1

9. The reflux ratio in the rectification column, (F_{30}).

Additionally, to ensure smooth solutions, penalizations for movements of decision variables between stages k

k and k+1are incorporated into the NMPC. The tuning parameters employed in the tracking objective function are as follows: $Q_1 = 1$; $R_1 = 0.05$; $R_2 = 0.05$; $R_3 = 0.05$; $R_4 = 0.05$; $R_5 = 0.05$; $R_6 = 0.05$; $R_7 = 0.05$; $R_8 = 0.05$; $R_9 = 0.05$; $R_{10} = 0.05$; $R_{11} = 0.05$; $P_1 = 0.01$; $P_2 = 0.01$; $P_3 = 0.01$; $P_4 = 0.01$; $P_5 = 0.01$; $P_6 = 0.01$; $P_7 = 0.01$; $P_8 = 0.01$; $P_9 = 0.01$; $P_{10} = 0.01$.

The actual plant is modeled by the dynamic nonlinear process developed in Aspen Dynamics. This study exclusively conducts simulation analyses, assuming a fully observable process.

Stage 6. Solution of the Stochastic-PWOC problem

The optimization problems delineated by equations (10) and (11) are solved utilizing a sequential approach. In both the optimization and regulatory layers, the decision variables undergo discretization through the application of a polynomial piecewise constant approximation.

To emulate realistic industrial conditions, the nominal operating parameters reported by [40] , were adopted as initial conditions. It is important to note that while the results may exhibit sensitivity to the chosen starting point, the employed metaheuristic algorithm for solving the optimization problem offers a significant advantage. By virtue of its stochastic nature, this algorithm facilitates the exploration of an expansive region within the domain of manipulated variables. Consequently, as elucidated by [57], this approach enhances the likelihood of identifying a near-global optimum solution.

The nonlinear dynamic model of the process, utilized for predicting future plant behavior and evaluating the efficacy of both optimization and regulatory layers, was developed using Aspen Dynamics, as elaborated in Section 3. The integration between this process model and the MATLAB optimization toolbox is facilitated through the AM Simulation Block in Simulink.

The seamless interconnection between Aspen Dynamics and MATLAB for addressing stochastic programming problems represents a significant advancement in PWOC, particularly when a rigorous dynamic nonlinear model of the process is requisite. This integration methodology enables a more comprehensive and accurate representation of complex industrial processes.

The operational workflow involves the transmission of discretized decision variables from MATLAB to the Aspen Dynamics model via the AM Simulation Block. This transfer mechanism allows for the subsequent evaluation of system states and the objective function within the high-fidelity Aspen Dynamics environment.

Here's a revised version of the text:

The bidirectional communication between the process model and optimization routine is crucial for iterative refinement. Specifically, state variables and model outputs are transmitted back to the MATLAB-based optimization algorithm. This feedback loop continues until a predetermined stopping criterion is satisfied, ensuring convergence to an optimal solution.

The optimization layer operates with a prediction horizon of 25 hours, a parameter chosen to balance computational efficiency with forecast accuracy. The optimization routine is invoked at regular intervals of 0.5 hours, providing frequent updates to the control strategy. Additionally, the system is designed to trigger an optimization call if the economic objective function experiences a decrease below a specified tolerance threshold.

The multistage Nonlinear Model Predictive Control (NMPC) layer operates with a prediction horizon of 2 hours, a parameter carefully selected to balance computational load with control performance. This layer is activated on a periodic basis every 0.2 hours, ensuring frequent updates to the control actions.

Furthermore, the system incorporates an event-triggered mechanism: the NMPC algorithm is also invoked when the controlled variables deviate from their optimal setpoints beyond a predefined tolerance. This dual activation strategy, combining time-based and deviation-based triggers, enables the control system to maintain tight regulation under normal operating conditions while also responding swiftly to significant process disturbances or setpoint changes.

5. S-PWOC for the Acrylic Acid Process: Results and Discussion

Preprints.org (www.preprints.org) | NOT PEER-REVIEWED | Posted: 4 September 2024 doi:10.20944/preprints202409.0351.v1

This section presents a comparative analysis of the proposed Stochastic PWOC approach against two alternative methodologies: the deterministic PWOC and the conventional PWC structure illustrated in Figure 1. The study evaluates three distinct scenarios, each addressing a specific type of uncertainty. Case 1 focuses on known process uncertainty, specifically the air temperature disturbance. Case 2 examines the impact of an unknown internal uncertainty, specifically a model parameter variation. Case 3 focuses on an unknown external uncertainty, namely fluctuations in the cost of the main product.

Case 1: Air temperature disturbance as known process uncertainty.

To assess the performance of three PWC architectures: Stochastic PWOC, Deterministic PWOC, and decentralized PWC, a process disturbance is introduced, a 10°C increase in air temperature at 0.4 hours. For clarity in subsequent figures, a consistent color scheme is employed: black denotes Stochastic PWOC results, blue represents Deterministic PWOC, and red indicates decentralized PWC outcomes.

Figure 4 illustrates the system response to known process uncertainty, depicting key process variables: air and propylene feeding profiles, reactor oxygen molar composition, reactor temperature, acrylic acid flowrate, and its molar composition at the rectification column bottoms. The Stochastic PWOC approach demonstrates optimal control by adjusting air flowrate (F_1) upwards and propylene flowrate (F_3) downwards, enhancing acrylic acid production (FAA-25). Notably, all control structures maintain the reactor's oxygen molar fraction (XO2-5) below 5% mol/mol, ensuring safe operation and mitigating explosion risks.

The Stochastic PWOC achieves the lowest reactor temperature (T_R), significantly enhancing the main reaction's selectivity. This optimization leads to increased acrylic acid production in the reactor, consequently improving the process economic profitability. All control structures exhibit satisfactory performance, with Stochastic and Deterministic PWOC approaches effectively tracking optimal temperature trajectories, while decentralized PWC maintains its predefined setpoint. Notably, all control structures consistently meet the acrylic acid molar fraction specification in the rectification column bottoms (XAA-25 > 0.995 mol/mol) throughout the entire time horizon.

Figure 5 illustrates key process indicators under known disturbances: economic profitability, azeotropic and rectification column bottom temperatures, and toluene makeup in the decanter. Table 5 reveals that the Stochastic PWOC approach achieves the highest cumulative profitability (1.7166 x10^5 USD), establishing it as the most economically advantageous control scheme among those evaluated.

The Deterministic PWOC approach ranks second in economic performance, achieving a cumulative profitability of 1.6274x10^5 USD. In contrast, the decentralized PWC control structure exhibits the least favorable economic outcome, with a cumulative profitability of 1.4158 x10^5 USD.

All analyzed control structures successfully maintain bottoms temperature constraints for both azeotropic and rectification columns throughout the entire time horizon, effectively preventing acrylic acid polymerization. Notably, the Stochastic PWOC achieves a significant reduction in toluene makeup (F_{19}), strategically minimizing raw material costs and thereby enhancing overall economic profitability.

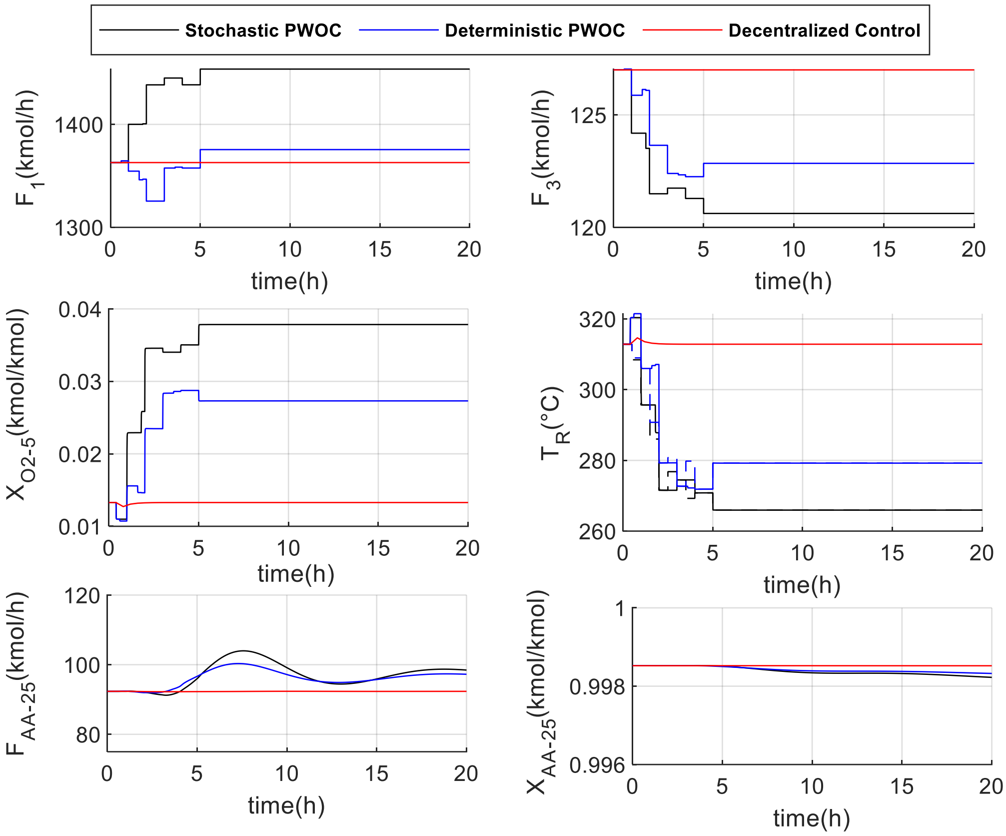

Figure 4. presents a comparative analysis of three (PWC) structures—Stochastic PWOC (black), Deterministic PWOC (blue), and Decentralized PWC (red)—under known process disturbance (Case 1). The figure illustrates six key process variables: air flowrate (top-left), propylene flowrate (top-right), reactor outlet oxygen molar fraction (middle-left), reactor temperature (middle-right), rectification column bottoms acrylic acid flowrate (bottom-left), and rectification column bottoms acrylic acid molar fraction (bottom-right).

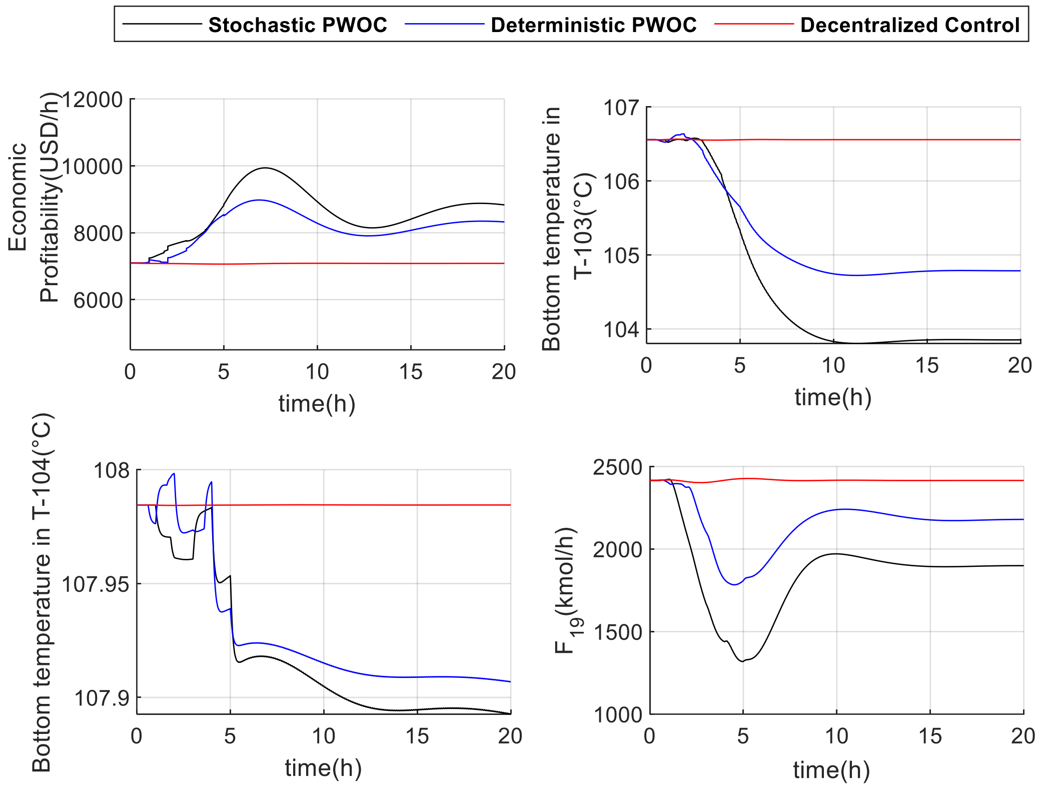

Figure 5. Comparison of the different PWC structures for the known process disturbance (Case 1): SPWOC (black), Deterministic PWOC (blue) and Decentralized PWC (red). Economic objective function (top-left), bottom temperature in azeotropic column (top-right), bottom temperature in rectification column (bottom-left), and toluene make up in decanter (bottom-right).

Table 5. Cumulative Profitability Comparison.

Tested Architecture.	**Cumulative Profitability (USD)**
Stochastic PWOC approach	1.7166 x10^5
Deterministic PWOC approach	1.6274 x10^5
Decentralized PWC approach	1.4158 x10^5

Case 2: Uncertainty related to a model parameter (activation energy E_{A1}): unknown internal uncertainty

Figure 6 illustrates key process parameters and outputs under conditions of unknown internal uncertainty. The figure presents: feeding profiles for air and propylene, oxygen molar composition in the reactor, reactor temperature, acrylic acid flowrate, acrylic acid composition at the bottom of the rectification column. These variables are shown to demonstrate system behavior in response to unknown internal uncertainties. The deterministic PWOC approach disregards uncertainty evolution, solving the optimization problem with a fixed nominal value for activation energy (E_{A1}).

The decentralized PWC approach, like its deterministic counterpart, ignores uncertainty evolution, focusing solely on maintaining controller variables at their set-points. In contrast, the Stochastic PWOC approach models uncertainty evolution using a scenario tree representation, with the optimization problem solved via equations (10)-(11).

The uncertainty in the simulated plant model is revealed after 0.4 hours, with extreme values from the scenario tree used to evaluate the performance of the analyzed control structures. The worst-case scenario, characterized by maximum activation energy (E_{A1}), leads to lower economic profitability, while the best-case scenario, with minimum E_{A1}, results in higher economic profitability.

The Stochastic PWOC approach employed a strategy of increasing air flowrate (F_1) while reducing propylene flowrate (F_3) to an optimal ratio. This method aimed to cool the reactor temperature (T_R) and enhance acrylic acid production ($F_{AA\text{-}25}$). In the best-case scenario, the Deterministic PWOC approach leads to safety constraint violations for reactor operation. Specifically, between 3-5 hours, the oxygen molar fraction in the reactor ($X_{O2\text{-}5}$) exceeds the 5% safety threshold.

This behavior is characteristic of deterministic approaches, which assume complete knowledge of model parameters. Such assumptions can lead to safety violations when uncertainties are present in the actual system. known [58–60]. When the optimizer of the model deviates from the actual plant conditions, constraint violations may arise [30]. However, all analyzed control structures maintain the molar fraction specification of acrylic acid in the rectification column bottoms (X_{AA25}>0.995 mol/mol).

Figure 6 illustrates the reactor temperature dynamics for the analyzed control structures. The decentralized control structure exhibits good performance in both best-case and worst-case scenarios. The Stochastic PWOC structure demonstrates reliable tracking of optimal temperature trajectories set by the optimization layer. In contrast, the Deterministic PWOC structure shows poor control performance in both extreme scenarios.

Figure 7 depicts four key performance indicators under conditions of unknown internal uncertainty: Economic profitability, bottom temperature in the azeotropic column, bottom temperature in the rectification column, toluene makeup in the decanter

Table 6. Comparative Analysis of Cumulative Profitability.

Tested Architecture	Cumulative Profitability (USD)
Stochastic PWOC approach	$1.6243x10^5$
Deterministic PWOC approach best case- scenario	$1.6259x10^5$
Deterministic PWOC approach worst-case scenario	$1.5966x10^5$
Decentralized Control worst-case scenario	$1.4139x10^5$
Decentralized Control best-case scenario	$1.4198x10^5$

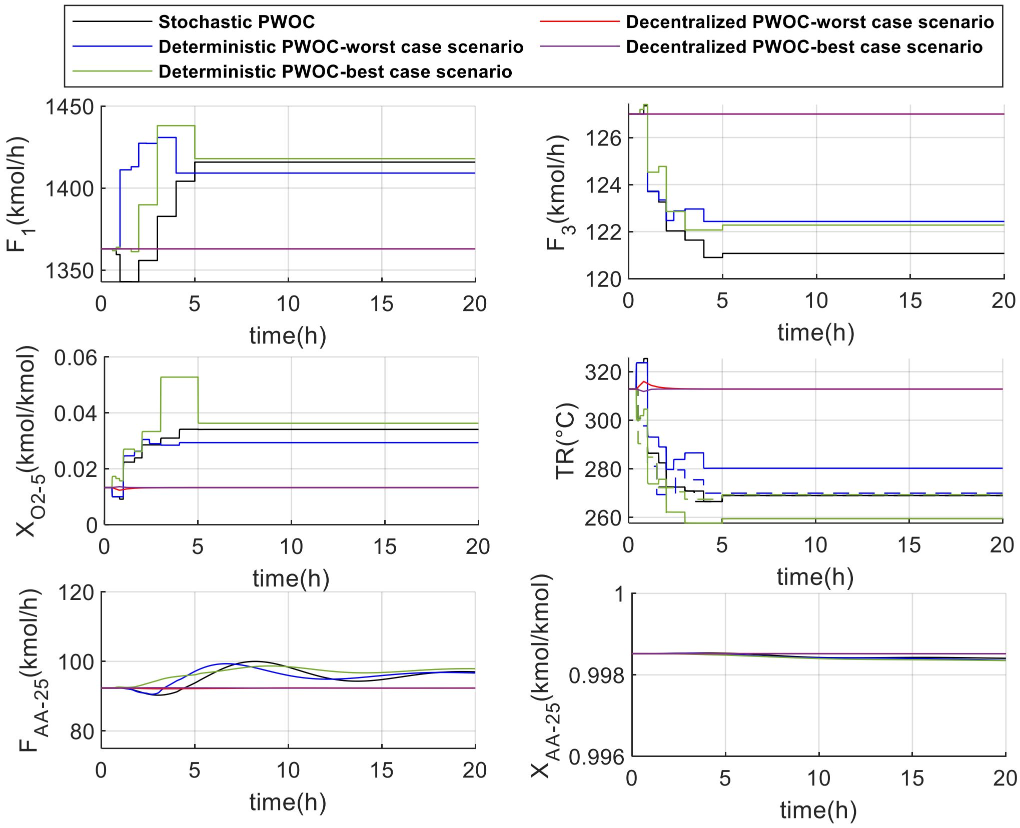

Figure 6. Comparison of the different PWC structures for the unknown internal uncertainty (Case 2): SPWOC (black), Deterministic PWOC (blue and green) and Decentralized PWC (red and magenta). Air flowrate (top-left), propylene flowrate (top-right), oxygen molar fraction at reactor outlet (middle-left), reactor temperature (middle-right), acrylic acid flowrate at bottoms rectification column (bottom-left) and acrylic acid molar fraction at bottoms rectification column (bottom-right).

Preprints.org (www.preprints.org) | NOT PEER-REVIEWED | Posted: 4 September 2024 doi:10.20944/preprints202409.0351.v1

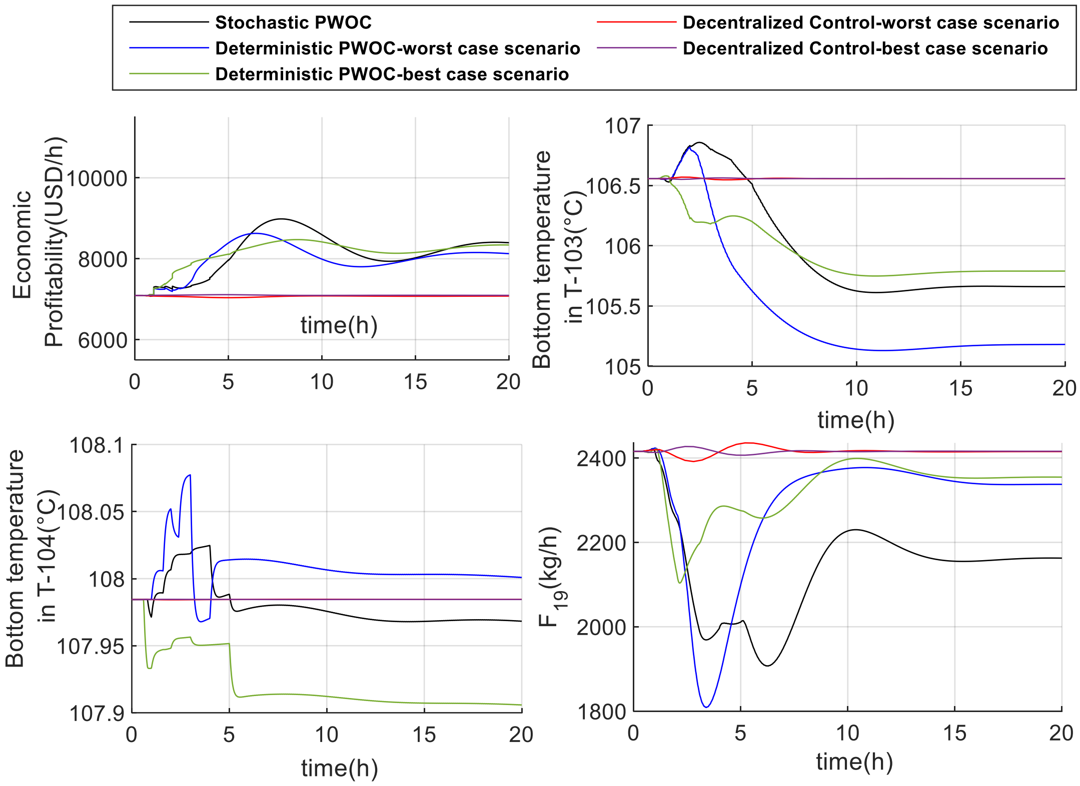

Figure 7. Comparison of the different PWC structures for the unknown internal uncertainty (Case 2): SPWOC (black), Deterministic PWOC (blue and green) and Decentralized PWC (red and magenta). Economic objective function (top-left), bottoms temperature in azeotropic column (top-right), bottoms temperature in rectification column (bottom-left), and toluene make up in decanter (bottom-right).

Case 3: Uncertainty in the acrylic acid price: unknown external uncertainty

Figures 8 and 9 compare the performance of the Stochastic PWOC approach against the Deterministic PWOC approach and decentralized PWC structure when an unknown disturbance in acrylic acid price affects the process. The uncertainty in the simulated plant model is revealed after 0.4 hours. Extreme values from the scenario tree are then used to evaluate the performance of the analyzed control structures. The worst-case scenario, characterized by minimum acrylic acid price, results in lower economic profitability. Conversely, the best-case scenario, with maximum acrylic acid price, leads to higher economic profitability. The safety constraint for reactor oxygen molar composition, $X_{O2\text{-}5}$ <5%mol/mol, was consistently met across the entire time horizon by all three analyzed PWC structures. Unlike model mismatches, market condition uncertainties did not impair constraint fulfillment in the deterministic approach. Both deterministic and stochastic PWOC approaches demonstrated effective reactor temperature control, accurately tracking optimal temperature trajectories. The deterministic PWOC approach achieves optimal state tracking performance because market conditions do not influence process state variables, and the optimizer calculates appropriate decision variables based on nominal model conditions. In the decentralized control structure, utility fluid flowrate remains constant as market disturbances do not affect process states, thus maintaining reactor temperature at its predefined steady-state value. The Deterministic PWOC (best-case scenario) and Stochastic PWOC approaches yield higher cumulative acrylic acid production (FAA-25), significantly enhancing the process economic profitability. Deterministic PWOC (worst-case) and decentralized PWC structures yield the lowest cumulative acrylic acid production, demonstrating their inability to mitigate negative market disturbances that adversely affect process profitability. However, all analyzed control structures maintain product specification (XAA-25) throughout the entire time horizon. Figure 9 illustrates economic profitability, bottoms

Preprints.org (www.preprints.org) | NOT PEER-REVIEWED | Posted: 4 September 2024 doi:10.20944/preprints202409.0351.v1

temperatures in azeotropic and rectification columns, and toluene makeup in the decanter under unknown external uncertainty. All control structures maintain bottoms temperatures below 110°C throughout the time horizon, ensuring safety constraints are met and preventing acrylic acid polymerization. The Stochastic PWOC structure achieves lower toluene makeup (F19), enhancing economic profitability. Table 7 reveals cumulative profitability rankings: Deterministic PWOC (best-case) leads at $1.7391x10^5$ USD, followed by Stochastic PWOC ($1.5855x10^5$ USD), decentralized control (best-case) at $1.5080x10^5$ USD, Deterministic PWOC (worst-case) at $8.2747x10^4$ USD, and decentralized control (worst-case) at $7.0264x10^4$ USD.

Table 7. Cumulative Profitability Comparison.

Tested Architecture.	Cumulative Profitability (USD)
Stochastic PWOC approach	$1.5855x10^5$
Deterministic PWOC approach worst-case scenario	$8.2747x10^4$
Deterministic PWOC approach best-case scenario	$1.7391x10^5$
Decentralized Control worst-case scenario	$7.0264x10^4$
Decentralized Control best-case scenario	$1.5080x10^5$

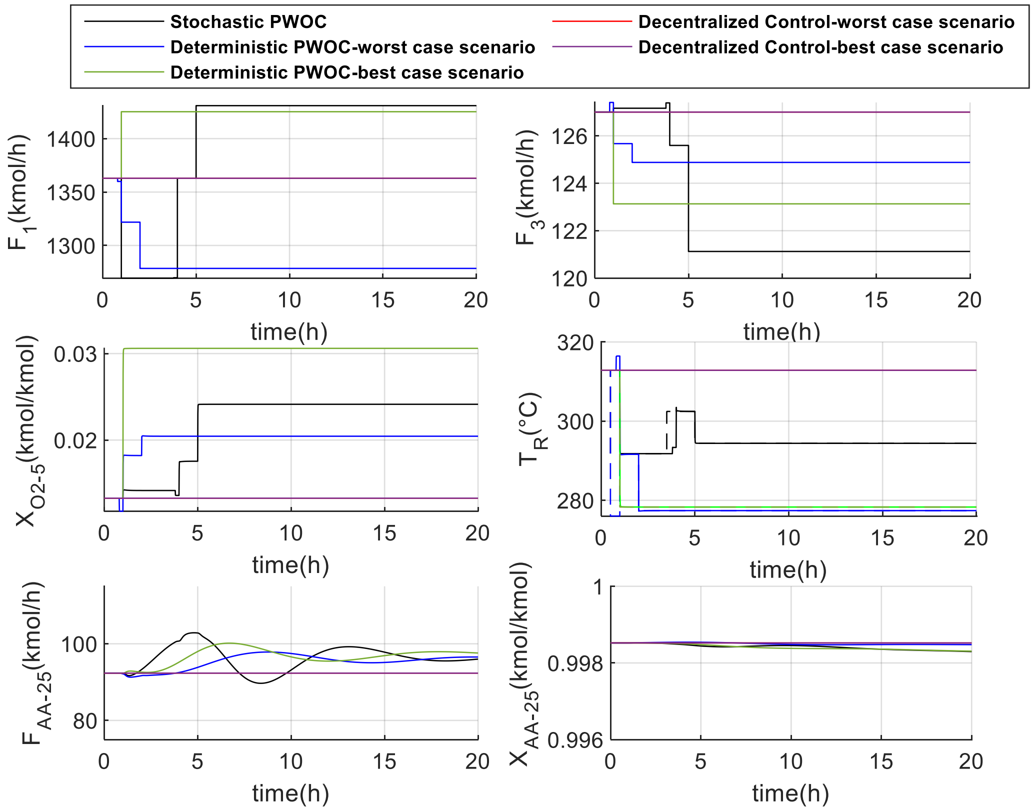

 doi:10.20944/preprints202409.0351.v1

Figure 8. Comparison of the different PWC structures for the unknown external uncertainty, acrylic acid price (Case 3): SPWOC (black), Deterministic PWOC (blue and green) and Decentralized PWC (red and magenta). Air flowrate (top-left), propylene flowrate (top-right), oxygen molar fraction at reactor outlet (middle-left), reactor temperature (middle-right), acrylic acid flowrate at bottoms rectification column (bottom-left) and acrylic acid molar fraction at bottoms rectification column (bottom-right).

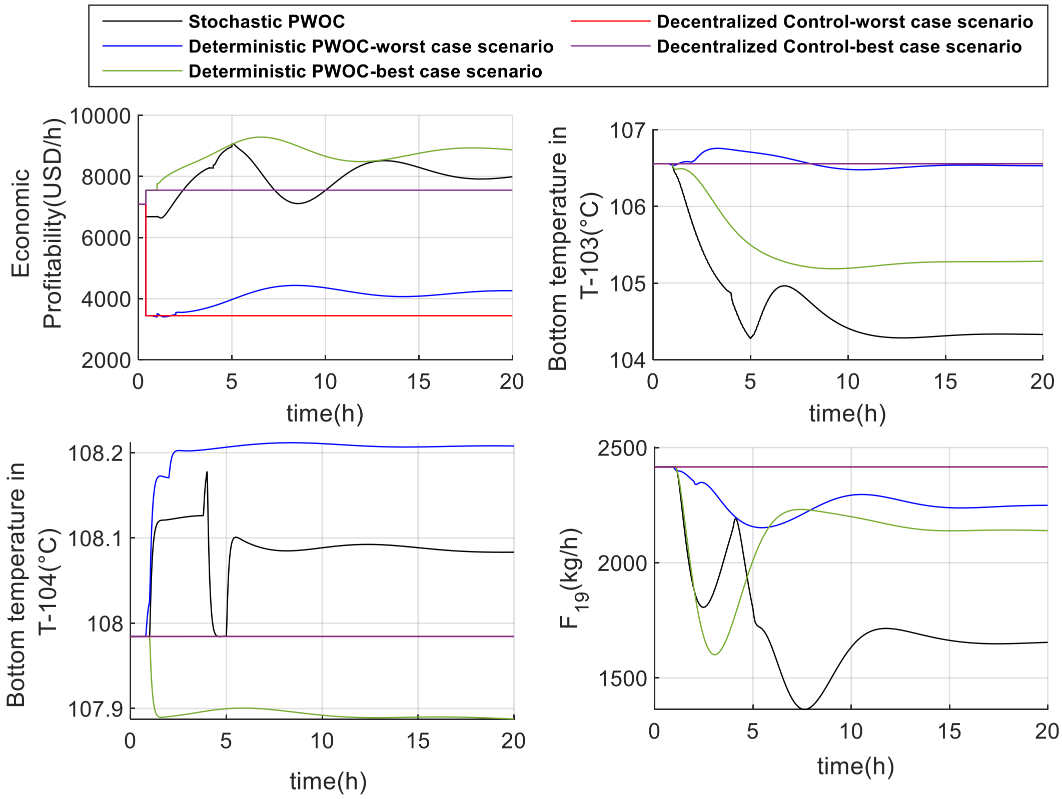

Figure 9. Comparison of the different PWC structures for the unknown external uncertainty, acrylic acid price (Case 3): SPWOC (black), Deterministic PWOC (blue and green) and Decentralized PWC (red and magenta). Economic objective function (top-left), bottoms temperature in azeotropic column (top-right), bottoms temperature in rectification column (bottom-left), and toluene make up in decanter (bottom-right).

6. Conclusions

The proposed Stochastic-Plantwide Optimizing Control (S-PWOC) methodology effectively manages uncertainties in acrylic acid plant control. Simulations demonstrate its superior performance in handling process, internal, and external uncertainties compared to Deterministic PWOC and decentralized control structures. S-PWOC achieves higher profitability, better state trajectory tracking, and ensures safe operation across all scenarios. However, its main limitation is increased computational time, particularly with numerous uncertain variables or complex scenario trees, potentially hindering real-time application. Parallel computing may mitigate this drawback.

Acknowledgments: Andrés Duque and Ricardo Tusso thank the economic support received from COLOMBIAN MINISTRY OF SCIENCE, TECHNOLOGY AND INNOVATION under the scholarships "Doctorados Nacionales-647". This research has been funded by Dirección General de Investigaciones of Universidad Santiago de Cali (CONV DGI 01-2023 proyecto No. 939-621123-237).

References

 doi:10.20944/preprints202409.0351.v1

1. Juliani Correa de Godoy, R.; Garcia, C. Plantwide Control: A Review of Design Techniques, Benchmarks, and Challenges. *Ind Eng Chem Res* **2017**, *56* (28), 7877–7887. https://doi.org/10.1021/acs.iecr.7b00416.
2. Wu, J.; Shang, S. Managing Uncertainty in AI-Enabled Decision Making and Achieving Sustainability. *Sustainability* **2020**, *12*, 8758. https://doi.org/10.3390/su12218758.
3. Lucia, S.; Andersson, J. A. E.; Brandt, H.; Diehl, M.; Engell, S. Handling Uncertainty in Economic Nonlinear Model Predictive Control: A Comparative Case Study. *J Process Control* **2014**, *24* (8), 1247–1259. https://doi.org/https://doi.org/10.1016/j.jprocont.2014.05.008.
4. Ochoa, S.; Wozny, G.; Repke, J. U. Plantwide Optimizing Control of a Continuous Bioethanol Production Process. In *Journal of Process Control*; 2010; Vol. 20, pp 983–998. https://doi.org/10.1016/j.jprocont.2010.06.010.
5. Duque, A.; Ochoa, S.; Odloak, D. Stochastic Multilayer Optimization for an Acrylic Acid Reactor. *ACS Omega* **2021**, *6* (40), 26150–26169. https://doi.org/10.1021/acsomega.1c03158.
6. *globenewswire.com*.
7. *ICIS.com web site*. https://www.icis.com/explore/.
8. Jean-Paul Lange. Production of Acrylic Acid. 20150353465, 2016.
9. Murthy Konda, N. V. S. N.; Rangaiah, G. P.; Krishnaswamy, P. R. Plantwide Control of Industrial Processes: An Integrated Framework of Simulation and Heuristics. *Ind Eng Chem Res* **2005**, *44* (22), 8300–8313. https://doi.org/10.1021/ie048951z.
10. Rangaiah, G. P.; Kariwala, V. *Plantwide Control: Recent Developments and Applications*; John Wiley and Sons Ltd, Ed.; United Kingdom, 2012.
11. Buckley, P. S. *Techniques of Process Control*; Wiley, Ed.; New York, 1964.
12. Scattolini, R. Architectures for Distributed and Hierarchical Model Predictive Control - A Review. *J Process Control* **2009**, *19* (5), 723–731. https://doi.org/10.1016/j.jprocont.2009.02.003.
13. Rawlings, J. B.; Stewart, B. T. Coordinating Multiple Optimization-Based Controllers: New Opportunities and Challenges. *J Process Control* **2008**, *18* (9), 839–845. https://doi.org/https://doi.org/10.1016/j.jprocont.2008.06.005.
14. Ochoa, S.; Wozny, G.; Repke, J. U. Plantwide Optimizing Control of a Continuous Bioethanol Production Process. In *Journal of Process Control*; Elsevier, 2010; Vol. 20, pp 983–998. https://doi.org/10.1016/j.jprocont.2010.06.010.
15. Pataro, I. M. L.; da Costa, M. V. A.; Joseph, B. Closed-Loop Dynamic Real-Time Optimization (CL-DRTO) of a Bioethanol Distillation Process Using an Advanced Multilayer Control Architecture. *Comput Chem Eng* **2020**, *143*, 1–14. https://doi.org/https://doi.org/10.1016/j.compchemeng.2020.107075.
16. Ravi, A.; Kaisare, N. S. A Multi-Objective Dynamic RTO for Plant-Wide Control. *IFAC-PapersOnLine* **2020**, *53* (1), 368–373. https://doi.org/https://doi.org/10.1016/j.ifacol.2020.06.062.
17. Morales-Rodelo, K.; Francisco, M.; Alvarez, H.; Vega, P.; Revollar, S. Collaborative Control Applied to BSM1 for Wastewater Treatment Plants. *Processes*. 2020, pp 2–22. https://doi.org/10.3390/pr8111465.
18. Ravi, A.; Kaisare, N. S. Two-Layered Dynamic Control for Simultaneous Set-Point Tracking and Improved Economic Performance. *J Process Control* **2021**, *97*, 17–25. https://doi.org/https://doi.org/10.1016/j.jprocont.2020.11.008.
19. Jahanshahi, E.; Krishnamoorthy, D.; Codas, A.; Foss, B.; Skogestad, S. Plantwide Control of an Oil Production Network. *Comput Chem Eng* **2020**, *136*, 1–14. https://doi.org/10.1016/j.compchemeng.2020.106765.
20. Mujiyanti, S. F.; Biyanto, T. R.; Pratama, I. P. E. W.; Kurniawan, I. A. The Control Design Optimization of Gas Processing Plant Based on Plantwide Control Method. *AIP Conf Proc* **2023**, *2580* (1), 40014. https://doi.org/10.1063/5.0122335.
21. Engell, S. Feedback Control for Optimal Process Operation. *J Process Control* **2007**, *17* (3), 203–219. https://doi.org/https://doi.org/10.1016/j.jprocont.2006.10.011.
22. Ricker, N.L. and Lee, J. H. Non-Linear Model-Predictive Control of the Tennessee Eastman Challenge Process. *Comput Chem Eng* **1995**, *19*, 961–981.
23. Aske, E. M. B.; Skogestad, S. Consistent Inventory Control. *Ind Eng Chem Res* **2008**, *48*, 10892–10902.
24. Assali, W.A. and McAvoy, T. Optimal Selection of Dominant Measurements and Manipulated Variables for Production Control. *Ind Eng Chem Res* **2010**, *49*, 7832–7842.
25. Garrido, J.; Vazquez, F.; Morilla, F. Centralized Multivariable Control by Simplified Decoupling. *J Process Control* **2012**, *22*, 1044–1062.
26. Duque, A.; Ochoa, S. Dynamic Optimization for Controlling an Acrylic Acid Process. In *2017 IEEE 3rd Colombian Conference on Automatic Control, CCAC 2017 - Conference Proceedings*; Institute of Electrical and Electronics Engineers Inc., 2017; Vol. 2018-Janua, pp 1–6. https://doi.org/10.1109/CCAC.2017.8276421.
27. G. E. P. Box. *Robustness in the Strategy of Scientific Model Building*; 1979.
28. Li, P.; Wendt, M.; Wozny, G. Optimal Production Planning for Chemical Processes under Uncertain Market Conditions. *Chem Eng Technol* **2004**, *27* (6), 641–651. https://doi.org/10.1002/ceat.200400048.

29. Navia, D.; Sarabia, D.; Gutiérrez, G.; Cubillos, F.; de Prada, C. A Comparison between Two Methods of Stochastic Optimization for a Dynamic Hydrogen Consuming Plant. *Comput Chem Eng* **2014**, *63*, 219–233. https://doi.org/10.1016/j.compchemeng.2014.02.004.
30. Lucia, S.; Finkler, T.; Engell, S. Multi-Stage Nonlinear Model Predictive Control Applied to a Semi-Batch Polymerization Reactor under Uncertainty. *J Process Control* **2013**, *23* (9), 1306–1319. https://doi.org/10.1016/j.jprocont.2013.08.008.
31. Müller, D.; Illner, M.; Esche, E.; Pogrzeba, T.; Schmidt, M.; Schomäcker, R.; Biegler, L. T.; Wozny, G.; Repke, J.-U. Dynamic Real-Time Optimization under Uncertainty of a Hydroformylation Mini-Plant. *Comput Chem Eng* **2017**, *106*, 836–848. https://doi.org/10.1016/J.COMPCHEMENG.2017.01.041.
32. Zhang, Q.; Cremer, J. L.; Grossmann, I. E.; Sundaramoorthy, A.; Pinto, J. M. Risk-Based Integrated Production Scheduling and Electricity Procurement for Continuous Power-Intensive Processes. *Comput Chem Eng* **2016**, *86*, 90–105. https://doi.org/https://doi.org/10.1016/j.compchemeng.2015.12.015.
33. Zeng, Z.; Cremaschi, S. Multistage Stochastic Models for Shale Gas Artificial Lift Infrastructure Planning. In *13 International Symposium on Process Systems Engineering (PSE 2018)*; Eden, M. R., Ierapetritou, M. G., Towler, G. P. B. T.-C. A. C. E., Eds.; Elsevier, 2018; Vol. 44, pp 1285–1290. https://doi.org/https://doi.org/10.1016/B978-0-444-64241-7.50209-3.
34. Al-Aboosi, F. Y.; El-Halwagi, M. M. A Stochastic Optimization Approach to the Design of Shale Gas/Oil Wastewater Treatment Systems with Multiple Energy Sources under Uncertainty. *Sustainability*. 2019. https://doi.org/10.3390/su11184865.
35. Chen, Y.; Lin, M.; Jiang, H.; Yuan, Z.; Chen, B. Optimal Design and Operation of Refinery Hydrogen Systems under Multi-Scale Uncertainties. *Comput Chem Eng* **2020**, *138*, 106822. https://doi.org/https://doi.org/10.1016/j.compchemeng.2020.106822.
36. Petsagkourakis, P.; Sandoval, I. O.; Bradford, E.; Galvanin, F.; Zhang, D.; Rio-Chanona, E. A. del. Chance Constrained Policy Optimization for Process Control and Optimization. *J Process Control* **2022**, *111*, 35–45. https://doi.org/https://doi.org/10.1016/j.jprocont.2022.01.003.
37. Sharma, K.; Singh, V. P.; Ebrahimnejad, A.; Chakraborty, D. Solving a Multi-Objective Chance Constrained Hierarchical Optimization Problem under Intuitionistic Fuzzy Environment with Its Application. *Expert Syst Appl* **2023**, *217*, 119595. https://doi.org/https://doi.org/10.1016/j.eswa.2023.119595.
38. Li, C.; Grossmann, I. E. A Review of Stochastic Programming Methods for Optimization of Process Systems Under Uncertainty. *Frontiers in Chemical Engineering* **2021**, *2*. https://doi.org/10.3389/fceng.2020.622241.
39. Turton, R.; Bailie, R. C.; Whiting, W. B.; Shaeiwitz, J. A.; Bhattacharyya, D. *Analysis, Synthesis, and Design of Chemical Processes*, Fouth.; Prentice Hall, Ed.; New York:, 2012. https://doi.org/10.1017/CBO9781107415324.004.
40. Suo, X.; Zhang, H.; Ye, Q.; Dai, X.; Yu, H.; Li, R. Design and Control of an Improved Acrylic Acid Process. *Chemical Engineering Research and Design* **2015**, *104*, 346–356. https://doi.org/10.1016/j.cherd.2015.08.022.
41. Luyben, W. L. Economic Trade-Offs in Acrylic Acid Reactor Design. *Comput Chem Eng* **2016**, *93*, 118–127. https://doi.org/10.1016/j.compchemeng.2016.06.005.
42. Luyben, W. L. Integrator / Deadtime Processes. *Ind. Eng. Chem. Res* **1996**, *35*, 3480–3483.
43. Luyben, W. L. Tuning Proportional - Integral Controllers for Processes with Both Inverse Response and Deadtime. *Ind. Eng. Chem. Res* **2000**, *39*, 973–976.
44. Ochoa, S.; Wozny, G.; Repke, J.-U. Plantwide Optimizing Control of a Continuous Bioethanol Production Process. *J Process Control* **2010**, *20*, 983–998.
45. Buckley, P. S. Techniques of Process Control. **1964**.
46. Shinskey, F. G. *Distillation Control: For Productivity and Energy Conservation*, 2nd ed.; McGraw-Hill, Ed.; New York, 1984.
47. Douglas, J. M. *Conceptual Design of Chemical Processes*; McGraw-, Hill, Eds.; New York, 1988.
48. Downs, J. J. Distillation Control in a Plantwide Control Environment. In *Practical Distillation Control*; Springer, New York, NY, 1992; pp 413–439. https://doi.org/10.1007/978-1-4757-0277-4_20.
49. Luyben, W. L.; Tyréus, B. D.; Luyben, M. L. *Plantwide Process Control*; McGraw-Hill, 1998.
50. Luyben, M. L.; Tyreus, B. D.; Luyben, W. L. Plantwide Control Design Procedure. *AIChE Journal* **1997**, *43* (12), 3161–3174. https://doi.org/10.1002/AIC.690431205.
51. Ganzer, G.; Freund, H. Kinetic Modeling of the Partial Oxidation of Propylene to Acrolein: A Systematic Procedure for Parameter Estimation Based on Non-Isothermal Data. *Industrial and Engineering Chemistry Research* **2019**, *58* (5), 1857–1874. https://doi.org/10.1021/acs.iecr.8b05583.
52. Engell, S. Online Optimizing Control: The Link between Plant Economics and Process Control. In *Computer Aided Chemical Engineering*; Elsevier B.V., 2009; Vol. 27, pp 79–86. https://doi.org/10.1016/S1570-7946(09)70234-2.
53. Lucia, S. Robust Multi-Stage Nonlinear Model Predictive Control, Dortmund, 2015.
54. López, D. A. N. Handling Uncertainties in Process Optimization, Valladolid University, 2012.

 doi:10.20944/preprints202409.0351.v1

55. Martí, R.; Lucia, S.; Sarabia, D.; Paulen, R.; Engell, S. Improving Scenario Decomposition Algorithms for Robust Nonlinear Model Predictive Control. *Computers and Chemical Engineering* **2015**, *79*, 30–45. https://doi.org/10.1016/j.compchemeng.2015.04.024.
56. Bradford, E.; Reble, M.; Bouaswaig, A.; Imsland, L. Economic Stochastic Nonlinear Model Predictive Control of a Semi-Batch Polymerization Reaction. *IFAC-PapersOnLine* **2019**, *52* (1), 667–672. https://doi.org/https://doi.org/10.1016/j.ifacol.2019.06.139.
57. Thirunavukkarasu, M.; Sawle, Y.; Lala, H. A Comprehensive Review on Optimization of Hybrid Renewable Energy Systems Using Various Optimization Techniques. *Renewable and Sustainable Energy Reviews* **2023**, *176*, 113192. https://doi.org/https://doi.org/10.1016/j.rser.2023.113192.
58. Rockafellar, R. T. *Optimization under Uncertainty*; University of Washington: Washington, 2001.
59. Wendt, M.; Li, P.; Wozny, G. Nonlinear Chance-Constrained Process Opti-Mization under Uncertainty. *Ind Eng Chem Res* **2002**, *41*, 3621–3629.
60. Louveaux, F.; Birge, J. R. *Introduction to Stochastic Programming.*, Second Edi.; Springer: New York, 2011.